IEEE Access
Multidisciplinary | Rapid Review | Open Access Journal

Received September 27, 2020, accepted October 9, 2020, date of publication October 14, 2020, date of current version November 18, 2020.

Digital Object Identifier 10.1109/ACCESS.2020.3030879

Reducing the Standstill Spacing and Duration of Safe Braking Control in Vehicle Platoons With Delays

YUN MENG[1], (Member, IEEE), AND ZHUOYUAN WANG[2]
[1]School of Electronic and Control Engineering, Chang'an University, Xi'an 710064, China
[2]School of Electronics and Information Engineering, Tongji University, Shanghai 201804, China

Corresponding author: Yun Meng (mengyun@chd.edu.cn)

This work was supported in part by the National Key Research and Development Program of China under Grant 2020YFB1600400; in part by the National Natural Science Foundation of China under Grant 61701044, Grant 61803041, and Grant 11705014; in part by the Key Research and Development Program of Shaanxi under Program 2019GY-037; in part by the Shaanxi Province Natural Science Basic Research Program of China under Grant 2019JQ-687; and in part by the Xi'an Science and Technology Project.

ABSTRACT Braking control, especially in an emergency, is a key technology that is needed to ensure safety in vehicle platoons. However, delays in vehicle platoons can severely affect braking control. This paper proposes an optimized braking control to reduce the standstill spacing and braking duration during delays so that a platoon will stop within a short time frame with a reduced length, thus improving road utilization while ensuring both inter-vehicle and in-vehicle safety. However, two challenges need to be addressed. First, due to the delay in car-following interactions and the nonlinearity of the control law, an analysis model is needed to quantize the duration and distance during an emergency braking with delays. Second, the optimization of these control parameters is an NP-hard problem. Therefore, delay differential equations are introduced to model the braking process, and a crossing criterion is introduced to establish the relationship between the control law and the braking process. The propositions of standstill spacing and braking duration are then derived based on the Runge-Kutta method. According to these criteria, a particle swarm optimization (PSO) based on a lexicographic method with a penalty function is introduced to provide a solution framework with polynomial complexity. Simulation results verify the accuracy of the braking modeling process. Moreover, the results verify the performance of the proposed algorithm and provide a reference for platoon control.

INDEX TERMS Braking control, delay, standstill spacing, duration.

I. INTRODUCTION

As an important component of intelligent transport systems (ITSs), platoon-based driving patterns have attracted significant attention and are characterized by advantages including increased road safety, improved road capacity, and the reduction of energy consumption [1]. Many communities are aimed at furthering this work, such as the SARTRE program, PATH research, the Grand Cooperative Driving Challenge (GCDC), Energy ITS, and SCANIA platooning [2].

Braking control, especially in an emergency, is a key technology in vehicle platoons and is critical to ensuring both inter-vehicle and in-vehicle safety. Regarding the former, to avoid rear-end collisions, vehicles must be kept at a safe distance from each other during braking. Regarding the latter, to avoid an overloaded braking capacity and injuries to passengers [3]–[5], deceleration must be limited under the permissible maximum value.

There are various types of delays existing in practical platoon systems, which can be divided into two categories according to the execution stages of the braking control process: signal acquisition delays and control parameter calculation delays. The first category mainly includes communication delays [6] and sensor delays [7], [8]. Communication delays are caused by information transmission and the queuing of data packets, which are restricted by wireless channel quality and spectrum bandwidth; this type of delay ranges from a few milliseconds to tens of milliseconds. Sensor delays are caused by measurement, data sampling, obstacle detection, ego-positioning, environmental perception, and classification factors. For vision measurement systems in particular, image processing also takes time. This type of delay

The associate editor coordinating the review of this manuscript and approving it for publication was Yan-Jun Liu.

can range from tens of milliseconds to hundreds of milliseconds. Delays due to the calculation of control parameters can range from a few milliseconds to hundreds of milliseconds.

Delays have a negative impact on vehicle driving control. For an individual vehicle, delayed information can impair its ability to maintain a desired velocity and position [9]. For a platoon, without a proper driving control design, the delayed information will spread from the leader to the followers, threatening stability and creating deviations from the desired control target [10]. For emergency braking control in particular, the urgent timing and reduced spacing can lead to a greater risk of collision, which calls for a more rigorous design to overcome delays.

To ensure braking safety for platoons experiencing delays, it is beneficial to increase the inter-vehicle distance and decrease the velocity, as these measures can provide adequate spacing and time. However, these adjustments will reduce road utilization. Therefore, this paper proposes an optimized braking control to reduce standstill spacing and braking duration during delays while guaranteeing safety. The platoon must stop within a short time frame when an emergency occurs, and the length of the platoon must be shortened after the platoon stops to improve road utilization. However, the distances between vehicles must be greater than a safe distance during the braking process to avoid collisions, and the vehicle decelerations must be less than the maximum permissible value to minimize the damage to cars and the impact on passengers, thus ensuring both inter-vehicle and in-vehicle safety. However, two challenges need to be addressed. First, due to the delay in car-following interactions and the nonlinearity of the control law, an analysis model is needed to quantize the duration and the decreasing distance during the elapsed braking control time frame with delays. Second, the optimization of these control parameters is an NP-hard problem. To address these challenges, the standstill spacing and duration are theoretically analyzed by delay differential equations (DDEs), and a multiobjective and multivariable particle swarm optimization (PSO) algorithm is designed.

The main contributions of this paper are summarized as follows:

1) An analytical expression of the braking process is first modeled using DDEs to embed the effect of delays;
2) A crossing criterion is introduced to establish the relationship between the control law and the braking process and to classify various braking scenarios;
3) The propositions of standstill spacing and braking duration are derived based on the Runge-Kutta method;
4) When considering delays, the standstill spacing and braking duration of the platoon are shortened during emergency braking to improve road utilization while ensuring both inter-vehicle and in-vehicle safety, and a solution framework with polynomial complexity is provided.

The remainder of this paper is organized as follows. Section II introduces related research. Section III presents the system model and the optimization problem. Section IV analyzes the standstill spacing and duration via the DDE method. Section V proposes a multiobjective and multivariable PSO to solve the optimization problem. Section VI reports the results of simulations to verify the performance improvement of the proposed algorithm. Finally, Section VII concludes this paper.

II. RELATED WORKS

Delays in vehicle platoons have recently attracted substantial research attention. Various control policies have been designed for diverse objectives under certain delays, such as the achievement of consensus [11], the robustness for formation changes and control [12], [13], the consensus of vehicles and their consistency with traffic flow theory [14], coping with the curves and slopes of roads [15], [16], and spacing [17]. There have also been several studies concerning the combination of control and delay bounds under stable conditions [6], [18]–[20].

As a key component of platoon management, braking can be classified into two categories: target stopping position (TSP) and emergency braking. Regarding the first category, Li *et al*. proposed an integral sliding-mode control, and Liu *et al*. utilized the force approach to achieve cooperative TSP braking control [21]–[23]; however, the restriction of deceleration was only considered in one of these works [21]. Although delay was not considered in these TSP problems, the requirements induced by the attainable deceleration and the negative effect of delays could be resolved by increasing the braking distance because the stopping position was given before braking. However, regarding the second category of braking, namely, emergency braking, delays will greatly increase urgency. In a previous study, an experimental platform and an actual-vehicle experiment were set up to evaluate emergency braking [24], but delay was not considered. Several works have considered delays in emergency braking [25]–[27]. For instance, Flores *et al*. [25] presented a cooperative collision avoidance system based on pedestrian prediction, in which delay was considered merely in the correction of velocity, and in-vehicle safety was ignored. Xu *et al*. [26] compared different communication information structures and contents to analyze the intrinsic relationships between coordination and communication in platoons and enhance platoon safety, including during slow and fast braking. Thunberg *et al*. [27] analyzed the platoon dynamics during emergency braking via packet loss probabilities and packet transmission delays. While the limitation of deceleration to guarantee in-vehicle safety was considered in these works, the effect of delays on braking was solely reflected in deriving the delay bounds to ensure safety [26], [27]. Unlike in the existing literature, in this paper, the control parameters are optimized to improve road utilization while guaranteeing safety, and delays in car-following interactions during braking control are considered.

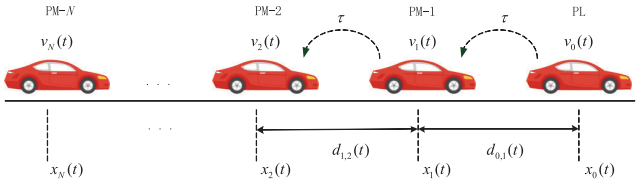

FIGURE 1. Predecessor-follower platoon model.

III. SYSTEM MODEL

A. PLATOON DESCRIPTION

As illustrated in Fig. 1, this paper considers a homogeneous platoon that includes a platoon leader (PL) and N platoon members (PMs). The length of each vehicle is denoted as L, the time variable is denoted as t, and the position of the i-th vehicle at time t is denoted as $x_i(t)$, where $i = 0$ is the PL and $i = \{1, 2, \ldots, N\}$ represents the PMs. It should be noted that the position of each vehicle is set as its center; thus, the distance between the centers of the (i-1)-th vehicle and i-th vehicle at time t, denoted as $d_{i-1,i}(t)$, can be obtained as $d_{i-1,i}(t) = x_{i-1}(t) - x_i(t)$. In addition, the velocity of the i-th vehicle at time t is denoted as $v_i(t)$, where $v_i(t) = x_i'(t)$.

In this paper, the information topology of platoon control is considered to be a predecessor-follower topology, in which each vehicle obtains the information from its predecessor, including the predecessor's velocity and position. The delay from the $(i-1)$-th vehicle to the i-th vehicle is denoted as τ. Here, delay τ is assumed to be time-invariant in this paper.

B. CONTROL MODEL

The optimal velocity model (OVM) is used in this paper, in which the acceleration or deceleration of the vehicle is determined by two aspects of the velocity difference, namely, the difference between the headway-dependent velocity and the actual velocity and the difference between the velocity of a given vehicle and the preceding vehicle [6], [28]. As a result, the control input (acceleration or deceleration) of the i-th PM, which is denoted as $u_i(t)$, is determined by the following control scheme [29]:

$$u_i(t) = a\left[V(d_{i-1,i}(t-\tau)) - v_i(t)\right] + b\left[v_{i-1}(t-\tau) - v_i(t)\right] \tag{1}$$

where a and b denote the associated gains of the aforementioned two aspects of the velocity difference. In addition, the headway-dependent velocity $V(d)$ is determined as follows [6], [28]:

$$V(d) = \begin{cases} 0 & \text{if } d < d_{\text{dense}} \quad (2a) \\ v_{\max} \times \left(\dfrac{d - d_{\text{dense}}}{d_{\text{sparse}} - d_{\text{dense}}}\right), & \text{if } d_{\text{dense}} \le d \le d_{\text{sparse}} \quad (2b) \\ v_{\max} & \text{if } d_{\text{sparse}} < d \quad (2c) \end{cases}$$

In a dense scenario, the vehicle will stop for the distance $d < d_{\text{dense}}$. In contrast, in a sparse scenario, the vehicle will travel with the maximum velocity, denoted as $v_{\max}$, when $d > d_{\text{sparse}}$. For $d_{\text{dense}} \le d \le d_{\text{sparse}}$, the desired velocity will increase linearly with d. The expression of $u_i(t)$ is nonlinear due to the nonlinearity of $V(d)$.

Assume that the maximum velocity $v_{\max}$ is a constant, and the original state of the platoon before braking is stable, i.e., $u_i(t) = 0$, $v_i(t) = v_{\text{stable}}$, and $d_{i-1,i}(t) = d_{\text{stable}}$. The relationship between d_{stable} and v_{stable} can be derived from Eqs. (1) and (2) as follows:

$$d_{\text{stable}} = v_{\text{stable}} \frac{d_{\text{sparse}} - d_{\text{dense}}}{v_{\max}} + d_{\text{dense}} \tag{3}$$

From an analysis of Eqs. (1) and (2), it can be found that, even for the same delay and the aforementioned two aspects of the velocity difference, different control parameters, including a, b, d_{dense} and d_{sparse}, will result in different braking processes. Hence, the control parameters must be optimized to improve road utilization while ensuring safety.

C. OPTIMIZATION PROBLEM STATEMENT

Consider a scenario in which the PL detects an emergency directly in front of the platoon, such as the crossing of a pedestrian or an obstacle on the highway. To obtain the theoretical mathematic expression, the braking of the PL is simplified as $v_0(t_{\text{start}}) = 0$, where t_{start} is the moment at which the PL stops immediately. It is reasonable to regard this as the most urgent case in braking. In addition, the string stability must be ensured so that the optimized parameters of PM1 can be extended to other following PMs [13], [30]. Thus, in the following description, $d_{0,1}(t) = d(t)$, $v_1(t) = v(t)$, $u_1(t) = u(t)$, $s_1(t) = s(t)$, $v_0(t) = v_{\text{stable}}$ if $t < t_{\text{start}}$, and $v_0(t) = 0$ if $t \ge t_{\text{start}}$, and $s(t) = -u(t)$, i.e., $s(t)$ represents deceleration and $s(t) \ge 0$.

Considering the effect of delay, to reduce the standstill spacing and the duration of braking while ensuring safety and string stability, the optimization problem is modeled as follows:

$$\begin{aligned} \text{P:} \quad & \min_{a,b,d_{\text{dense}},d_{\text{sparse}}} d_{\text{end}} \\ & \min_{a,b,d_{\text{dense}},d_{\text{sparse}}} t_{\text{end}} \\ s.t. \quad & \begin{cases} d(t) \ge d_{\text{safe}} & \text{(a)} \\ s(t) \le s_{\max} & \text{(b)} \\ a + 2b - 2 \ge 0 & \text{(c)} \\ a^2 + b^2 2ab - 4a \ge 0 & \text{(d)} \\ \dfrac{(a+2b)\left(d_{\text{sparse}} - d_{\text{dense}}\right) - 2v_{\max}}{2v_{\max}(a+b)} \ge \tau & \text{(e)} \end{cases} \end{aligned} \tag{4}$$

where d_{end} is denoted as the standstill spacing, i.e., the final distance at the end of braking, t_{end} is the entire duration of braking, d_{safe} is the safe distance to avoid a rear-end collision, and $s_{\max}$ is the safe permissible maximum value of deceleration to avoid damage to the vehicle structures and endangering passenger safety. In the optimization problem **P**, there are two optimization objectives for reducing

the standstill spacing and the braking duration. Constraints (a) and (b) ensure inter-vehicle safety and in-vehicle safety, respectively. Constraints (c), (d), and (e) ensure the string stability of the platoon, where $\frac{(a+2b)(d_{\text{sparse}}-d_{\text{dense}})-2v_{\max}}{2v_{\max}(a+b)} = \tau_{\text{string}}$ is the maximum permissible delay to ensure the string stability of a platoon with the control law in Eq. (1) [6]. Thus, the optimization of $\mathbf{P}$ is based on the string stability of the platoon, which is guaranteed by constraints (c-e).

It is difficult to solve this optimization problem. On the one hand, due to the delay in the car-following interactions and the nonlinearity of the control law, there is no analysis model that can quantize the duration and the decreasing distance in the elapsed time of braking control. On the other hand, the optimization of these control parameters is an NP-hard problem, and a solution framework with low computational complexity must be provided. These two challenges are addressed in Sections IV and V.

IV. ANALYSIS OF STANDSTILL SPACING AND BRAKING DURATION BY DDEs

To analyze the final standstill spacing d_{end} and braking duration t_{end}, an overview analysis of two braking scenarios and the reason for their existence are presented in subsection IV-A. Then, subsection IV-B proposes a crossing criterion for judging to which scenario the braking process belongs. Then, in subsection IV-C, the time functions $d(t)$ and $v(t)$ are analyzed. Finally, the final standstill spacing d_{end} and braking duration t_{end} are derived in subsection IV-D.

A. ANALYSIS OF THE BRAKING PROCESS

Beginning at t_{start}, PM1 will continue driving at v_{stable} until $t = t_{\text{start}}+\tau$ due to the existence of the delay τ, and this phase is defined as Delay phase. Then, PM1 starts to enter Braking phase, during which its starting moment is denoted as t_{brake}, i.e., $t_{\text{brake}} = t_{\text{start}} + \tau$. Here, $t_{\text{brake}} = 0$ for the convenience of the analysis of the DDE in subsection IV-B; thus, $t_{\text{start}} = -\tau$. During Braking phase, $v(t)$ and $d(t)$ decrease continuously from v_{stable} and d_{stable} with t until $v(t) = 0$. In addition, the range of d_{stable} can be derived as $d_{\text{dense}} \le d_{\text{stable}} \le d_{\text{sparse}}$ from Eqs. (1) and (2). Thus, there are two types of braking stages based on Eq. (2), and their control laws are as follows.

Braking stage 1:

$$\begin{aligned} u(t) &= a\left[V(d(t-\tau))-v(t)\right]+b\left[v(t-\tau)-v(t)\right] \\ V(d(t-\tau)) &= v_{\max}\times\left(\frac{d(t-\tau)-d_{\text{dense}}}{d_{\text{sparse}}-d_{\text{dense}}}\right), \\ &\quad \text{if } d_{\text{dense}} \le d(t-\tau) \le d_{\text{stable}} \end{aligned} \tag{5}$$

Braking stage 2:

$$\begin{aligned} u(t) &= a\left[V(d(t-\tau))-v(t)\right]+b\left[v(t-\tau)-v(t)\right] \\ V(d(t-\tau)) &= 0, \quad \text{if } d(t-\tau) < d_{\text{dense}} \end{aligned} \tag{6}$$

Based on whether $v(t)$ has reduced to 0 in Braking stage 1, the braking process can be classified into Braking scenario 1 and Braking scenario 2.

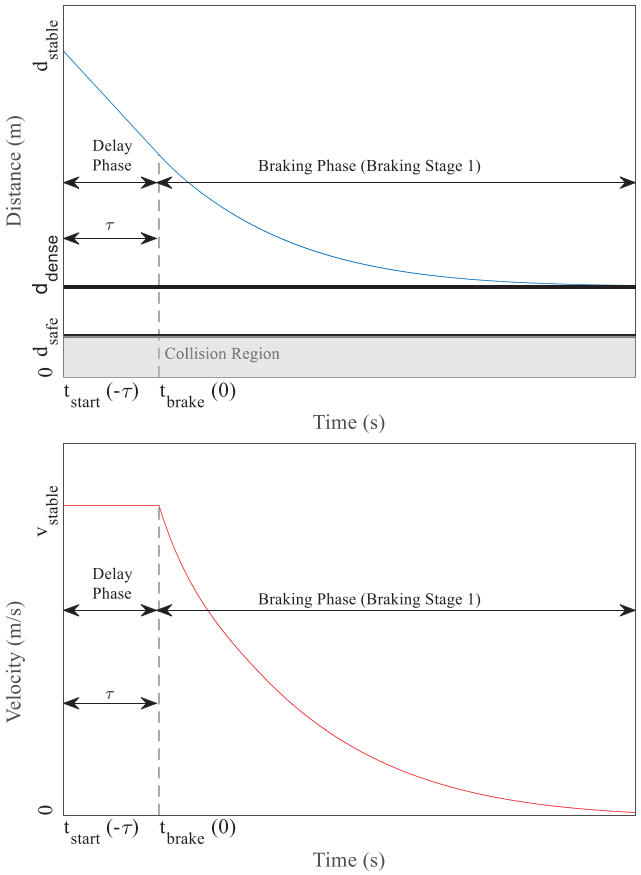

FIGURE 2. Braking scenario 1.

1) BRAKING SCENARIO 1

As presented in Fig. 2, in Braking scenario 1, PM1 experiences Delay phase and Braking stage 1 and finally stops in Braking stage 1.

First, the expressions of $d(t)$ and $v(t)$ in Delay phase are as follows.

$$d(t) = d_{\text{stable}} - v_{\text{stable}}(t+\tau), \quad -\tau \le t \le 0 \tag{7a}$$

$$v(t) = v_{\text{stable}}, \quad -\tau \le t \le 0 \tag{7b}$$

Then, in Braking phase, PM1 will brake with the control law of Braking stage 1. Thus, by substituting Eq. (2b) into Eq. (1), the expressions of $u(t)$ and $d(t)$ can be derived as follows.

$$\begin{cases} u(t) = a\left(v_{\max}\dfrac{d(t-\tau)-d_{\text{dense}}}{d_{\text{sparse}}-d_{\text{dense}}}\right) \\ -(a+b)v(t) \\ \Rightarrow d''(t) + \dfrac{av_{\max}d(t-\tau)}{d_{\text{sparse}}-d_{\text{dense}}} \\ +(a+b)d'(t) = \dfrac{av_{\max}d_{\text{dense}}}{d_{\text{sparse}}-d_{\text{dense}}}, \\ \qquad \text{if } t > 0 \text{ and } d_{\text{dense}} \le d(t-\tau) \le d_{\text{stable}} \end{cases} \tag{8}$$

It can be seen that Eq. (8) is a DDE with delay τ. The analysis of Eq. (8) is presented in subsection IV-C.

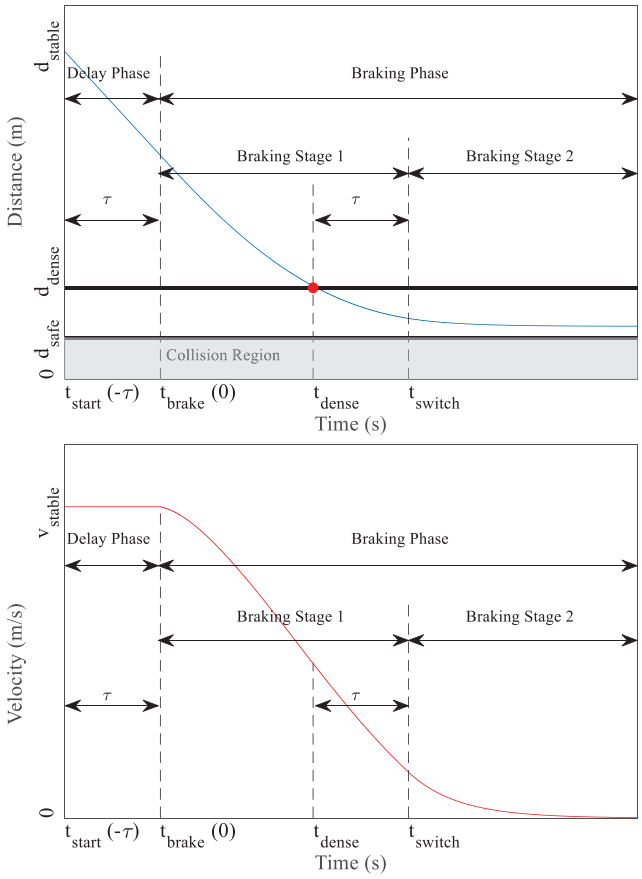

FIGURE 3. Braking scenario 2.

2) BRAKING SCENARIO 2

As presented in Fig. 3, in Braking scenario 2, PM1 experiences Delay phase, Braking stage 1, and Braking stage 2, and it finally stops in Braking stage 2.

In Braking scenario 2, as shown in Fig. 3, the red dot denotes that $d(t) = d_{\text{dense}}$, and this moment is denoted as t_{dense}. Due to the existence of delay τ, the control law will switch to Braking stage 2 at $t_{\text{wsitch}} = t_{\text{dense}} + \tau$. As Delay phase and Braking stage 1 are the same as those in Braking scenario 1, Braking stage 2 is subsequently analyzed.

The equation of $d(t)$ in Braking stage 2 is derived by substituting Eq. (2a) into Eq. (1), as follows:

$$\begin{cases} u(t) = -(a+b)v(t) \\ \Rightarrow d''(t) + (a+b)d'(t) = 0, \end{cases} \quad \text{if } t \geq t_{\text{switch}}. \tag{9}$$

It can be seen that Eq. (9) is an ordinary differential equation (ODE) without any delay. Thus, the solution of Eq. (9) is

$$d(t) = C_1 e^{-(a+b)t} + C_2. \tag{10}$$

The initial conditions of Eq. (10) are $d(t_{\text{wsitch}}) = d_{\text{wsitch}}$ and $d'(t_{\text{wsitch}}) = -v_{\text{wsitch}}$. It should be noted that the values of d_{wsitch} and v_{wsitch} can be obtained as the final values of Braking stage 1.

By substituting the initial conditions into Eq. (9), the expressions of $d(t)$ and $v(t)$ in Braking stage 2 are derived as:

$$d(t) = \left(\frac{v_{\text{switch}} e^{(a+b)t_{\text{switch}}}}{a+b}\right) e^{-(a+b)t} + \left(d_{\text{switch}} - \frac{v_{\text{switch}}}{a+b}\right), \quad t \geq t_{\text{switch}}, \tag{11a}$$

$$v(t) = -d'(t) = v_{\text{switch}} e^{(a+b)(t_{\text{switch}}-t)}, \quad t \geq t_{\text{switch}}. \tag{11b}$$

Based on the preceding analysis, the braking processes for both braking scenarios are modeled. In subsection IV-B, the crossing criterion for judging whether the braking process belongs to Braking scenario 1 or Braking scenario 2 is presented.

B. CROSSING CRITERION FOR DIFFERENTIATING BRAKING SCENARIOS

As revealed by the analysis of the braking process based on Figs. 2 and 3, $d(t) = d_{\text{dense}}$ is the condition for judging which braking scenario the braking process belongs to. The equivalence substitution is then conducted as follows:

$$r(t) = d(t) - d_{\text{dense}}, \tag{12a}$$

$$r(t-\tau) = d(t-\tau) - d_{\text{dense}}. \tag{12b}$$

The judgment of $d(t) = d_{\text{dense}}$ can then be transformed into the judgment of $r(t) = 0$. By deriving two sides of Eq. (12a), the following can be obtained:

$$r'(t) = d'(t) \tag{13}$$

Then, by substituting Eqs. (12b) and (13) into Eq. (5), the following can be obtained:

$$r''(t) + \frac{a v_{\max}}{d_{\text{sparse}} - d_{\text{dense}}} r(t-\tau) + (a+b)r'(t) = 0, \quad \text{if } 0 \leq r(t) \leq d_{\text{sparse}} - d_{\text{dense}} \text{ and } t > 0 \tag{14}$$

Here, $r(t)$ has the following form if the solution of Eq. (14) is nonoscillatory and decreasing [31]:

$$r(t) = Ae^{-zt} \tag{15}$$

where z is a positive number greater than 0.

Substitute $r(0) = d(0) - d_{\text{dense}} = d_{\text{stable}} - v_{\text{stable}}\tau - d_{\text{dense}}$ and $d_{\text{stable}} = v_{\text{stable}} \frac{d_{\text{sparse}} - d_{\text{dense}}}{v_{\max}} + d_{\text{dense}}$ into Eq. (15) to obtain the value of A. Then, by substituting the value of A into Eq. (15) and Eq. (12a), the expressions of $r(t)$ and $d(t)$ are

$$r(t) = v_{\text{stable}} \left(\frac{d_{\text{sparse}} - d_{\text{dense}}}{v_{\max}} - \tau\right) e^{-zt} \tag{16}$$

$$d(t) = v_{\text{stable}} \left(\frac{d_{\text{sparse}} - d_{\text{dense}}}{v_{\max}} - \tau\right) e^{-zt} + d_{\text{dense}} \tag{17}$$

If the solution to Eq. (14) is nonoscillatory and decreasing, $r(t)$ will never cross $r = 0$, i.e., this braking process will belong to Braking scenario 1; otherwise, it will belong to Braking scenario 2. Thus, the following crossing criterion is defined.

Crossing criterion: The braking process is Braking scenario 1, i.e., the solution of Eq. (13) *is nonoscillatory and decreasing if the following inequality is satisfied:*

$$f(z_0) = z_0^2 - (a+b)z_0 + \frac{av_{\max}}{d_{\text{sparse}} - d_{\text{dense}}} e^{-z_0\tau} \le 0, \quad (18)$$

where $z_0 = (a+b)/2 + W(0, a\tau^2 v_{\max} e^{-(a+b)\tau/2}/2(d_{\text{sparse}} - d_{\text{dense}}))/\tau$ *and* $W(.)$ *denotes the inverse function of* $f(x) = xe^x$.

Proof: The following can be obtained by the first and second derivatives of Eq. (15):

$$r'(t) = -zAe^{-zt}, \quad (19)$$
$$r''(t) = z^2 Ae^{-zt}. \quad (20)$$

By substituting Eqs. (15), (19), and (20) into Eq. (14), Eq. (14) is transformed by simplification as follows:

$$z^2 - (a+b)z + \frac{av_{\max}}{d_{\text{sparse}} - d_{\text{dense}}} e^{-z\tau} = 0. \quad (21)$$

As a result, the *crossing criterion* is transformed into the existence of a positive z in Eq. (21) [31], [32].

However, Eq. (21) is a transcendental equation, and the analytic solution of z cannot be obtained; therefore, the proposition is transformed into the existence of a positive zero-point of $f(z)$, where

$$f(z) = z^2 - (a+b)z + \frac{av_{\max}}{d_{\text{sparse}} - d_{\text{dense}}} e^{-z\tau}. \quad (22)$$

The first derivative of $f(z)$ is

$$f'(z) = 2z - (a+b) - \tau \frac{av_{\max}}{d_{\text{sparse}} - d_{\text{dense}}} e^{-z\tau}. \quad (23)$$

Observably, $f(0) > 0, f'(0) < 0$, and $f'(+\infty) \to +\infty$, and $f'(z)$ increases monotonically, i.e., $f'(z)$ only has one positive zero-point and $f(z)$ has a minimum value for $z > 0$. Hence, the positive zero-point z_0 of $f'(z)$ is

$$z_0 = \frac{a+b}{2} + \frac{W\left(0, \frac{a\tau^2 v_{\max} e^{-\frac{(a+b)\tau}{2}}}{2(d_{\text{sparse}} - d_{\text{dense}})}\right)}{\tau}, \quad (24)$$

where $W(.)$ is the inverse function of $f(x) = xe^x$.

$f(z_0)$ is the minimum value of $f(z)$ so that $f(z)$has one positive zero-point only if $f(z_0) \le 0$, i.e.,

$$f(z_0) = z_0^2 - (a+b)z_0 + \frac{av_{\max}}{d_{\text{sparse}} - d_{\text{dense}}} e^{-z_0\tau} \le 0. \quad (25)$$

The conclusion can be drawn that the DDE (14) is non-crossing and decreasing, i.e., the braking process is Braking scenario 1, if Eqs. (24) and (25) are satisfied.

The *crossing criterion* comprises a, b, $v_{\max}$, d_{dense}, and d_{sparse}, and is not related to v_{stable}; in other words, a, b, $v_{\max}$, d_{dense}, and d_{sparse} determine whether the braking process belongs to Braking scenario 1 or 2.

C. TIME FUNCTIONS OF DISTANCE AND VELOCITY IN THE BRAKING PROCESS

In Sections IV-A and IV-B, it can be seen that there are two types of braking scenarios, namely Braking scenario 1 and Braking scenario 2, and both consist of Delay phase and Braking phase. The difference between the two braking scenarios is the element of Braking phase; there exists only Braking stage 1 for Braking scenario 1 while the additional Braking stage 2 is included for Braking scenario 2. The time function of distance (velocity) in Braking scenario 1 is a piecewise function of two segments, while that for Braking scenario 2 is a piecewise function of three segments, in which the former two segments are the same as those in Braking scenario 1. It should be noted that the value of the end-point of each segment is the initial value of the following segment. The time functions of all the segments are subsequently presented.

1) TIME FUNCTIONS OF DISTANCE AND VELOCITY IN DELAY PHASE

For compactness of expression and the benefit of substitution in the subsequent segments, $d(t)$ and $v(t)$ are equivalently transformed into the matrix form based on Eqs. (7a) and (7b):

$$\mathbf{y} = \mathbf{P}t + \mathbf{Q}, \quad -\tau \le t \le 0 \quad (26)$$

where

$$\mathbf{y} = \begin{bmatrix} d(t) \\ v(t) \end{bmatrix}, \quad \mathbf{P} = \begin{bmatrix} -v_{\text{stable}} \\ 0 \end{bmatrix}, \quad \mathbf{Q} = \begin{bmatrix} d_{\text{stable}} - v_{\text{stable}}\tau \\ v_{\text{stable}} \end{bmatrix}$$

2) TIME FUNCTIONS OF DISTANCE AND VELOCITY IN BRAKING STAGE 1

Based on Eqs. (5) and (8), the expressions of $d'(t)$ and $v'(t)$ in Braking stage 1 can be transformed into the following matrix form:

$$\mathbf{y}' = \mathbf{L}\mathbf{y} + \mathbf{M}\mathbf{s} + \mathbf{N}, \quad t > 0, \quad (27)$$

where

$$\mathbf{L} = \begin{bmatrix} 0 & -1 \\ 0 & -(a+b) \end{bmatrix}, \quad \mathbf{M} = \begin{bmatrix} 0 & 0 \\ \frac{av_{\max}}{d_{\text{sparse}} - d_{\text{dense}}} & 0 \end{bmatrix},$$
$$\mathbf{N} = \begin{bmatrix} 0 \\ -a\frac{d_{\text{dense}} v_{\max}}{d_{\text{sparse}} - d_{\text{dense}}} \end{bmatrix}, \quad \mathbf{S} = \begin{bmatrix} d(t-\tau) \\ v(t-\tau) \end{bmatrix}.$$

It can be seen that Eq. (27) is a set of DDEs, and the Runge-Kutta method with four orders (RK4) is introduced to obtain the approximate solution with high precision in this paper, the time step of which is denoted as Δt. It can be determined from Eq. (27) that as $d(t)$ and $v(t)$ are related to the state of τ prior to t in Braking stage 1, the values of $d(t)$ and $v(t)$ in Eq. (26) must be obtained at the steps in Delay phase.

Proposition 1: In Delay phase, the values of $d(t)$ and $v(t)$ of each point in Δt of PM1 can be obtained as follows:

$$\mathbf{y}_n = \begin{bmatrix} d_n \\ v_n \end{bmatrix} = \begin{bmatrix} d_{\text{stable}} - v_{\text{stable}}\tau - n\Delta t v_{\text{stable}} \\ v_{\text{stable}} \end{bmatrix},$$
$$t_n = n\Delta t, \quad n = -\frac{\tau}{\Delta t}, \ldots, 0 \quad (28)$$

where t_n denotes the n-th point of Δt, while $\mathbf{y}_n$, d_n, and v_n respectively represent the approximate values of $\mathbf{y}$, $d(t)$, and $v(t)$ at t_n.

The time functions of $d(t)$ and $v(t)$ in Braking stage 1 can then be derived based on RK4 [33] by substitution in Eq. (27), which is represented as *Proposition 2*.

Proposition 2: In Braking stage 1, the distance and velocity of PM1 are approximately obtained as follows:

$$\begin{aligned}
\mathbf{y}_{n+1} &= \mathbf{y}_n + \frac{\Delta t}{6}(\mathbf{k}_{n,1} + 2\mathbf{k}_{n,2} + 2\mathbf{k}_{n,3} + \mathbf{k}_{n,4}) \\
\mathbf{k}_{n,1} &= \mathbf{L}\mathbf{y}_n + \mathbf{M}\mathbf{y}_{n-q} + \mathbf{N} \\
\mathbf{k}_{n,2} &= \mathbf{L}\left(\mathbf{y}_n + \frac{\Delta t}{2}\mathbf{k}_{n,1}\right) + \mathbf{M}\left(\mathbf{y}_{n-q} + \frac{\Delta t}{2}\mathbf{k}_{n-q,1}\right) + \mathbf{N} \\
\mathbf{k}_{n,3} &= \mathbf{L}\left(\mathbf{y}_n + \frac{\Delta t}{2}\mathbf{k}_{n,2}\right) + \mathbf{M}\left(\mathbf{y}_{n-q} + \frac{\Delta t}{2}\mathbf{k}_{n-q,2}\right) + \mathbf{N} \\
\mathbf{k}_{n,4} &= \mathbf{L}\mathbf{y}(\mathbf{y}_n + \Delta t\mathbf{k}_{n,3}) + \mathbf{M}(\mathbf{y}_{n-q} + \Delta t\mathbf{k}_{n-q,3}) + \mathbf{N} \\
t_n &= n\Delta t, \\
q &= \frac{\tau}{\Delta t} \\
n &= 0, 1, 2, \ldots
\end{aligned} \tag{29}$$

where $\mathbf{k}_{n,i}$ denotes the i-th approximate growth rate of $\mathbf{y}_n$. In addition, $\mathbf{k}_{n,i} = d\left(\mathbf{P}(n\Delta t) + \mathbf{Q}\right)/dt (n \leq 0, i = 1, 2, 3)$ and the value of $\mathbf{y}_n (n \leq 0)$ is obtained by Proposition 1.

Proof: Please see the proof for *Proposition 2* in the Appendix. □

3) TIME FUNCTIONS OF DISTANCE AND VELOCITY IN BRAKING STAGE 2

For Braking scenario 2, Braking stage 2 follows Braking stage 1. Based on the preceding analysis of the time functions of $d(t)$ and $v(t)$ in Braking stage 1, their values at the end of Braking stage 1 can be obtained as d_{switch} and v_{switch}, respectively. Then, by substituting them into Eqs. (11a) and (11b), the time functions of $d(t)$ and $v(t)$ in Braking stage 2 can be derived.

D. STANDSTILL SPACING AND BRAKING DURATION

Based on the time functions analyzed in Section IV-C, the standstill spacing d_{end} and braking duration t_{end}, which are the values of $d(t)$ and t when PM1 stops, are obtained. In this paper, PM1 is considered to stop if $v(t) \leq \varepsilon$, where ε is a relatively small constant. The values of d_{end} and t_{end} in Braking scenarios 1 and 2 are then derived by *Propositions 3* and *4*, respectively.

Proposition 3: The values of d_{end} and t_{end} in Braking scenario 1 are obtained as follows:

$$\begin{aligned}
d_{\text{end}} &= d_{\text{dense}} \\
t_{\text{end}} &= \min_{n:v_n \leq \varepsilon} n\Delta t
\end{aligned} \tag{30}$$

Proof: Please see the proof for *Proposition 3* in the Appendix. □

Proposition 4: The values of d_{end} and t_{end} in Braking scenario 2 are obtained as follows:

$$\begin{aligned}
d_{\text{end}} &= d_{\text{switch}} - \frac{v_{\text{switch}}}{a+b} \\
t_{\text{end}} &= \begin{cases} t_{\text{switch}} + \dfrac{\ln v_{\text{switch}} - \ln \varepsilon}{a+b}, & \text{if } v_{\text{switch}} \geq \varepsilon \\ \min\limits_{n:v_n \leq \varepsilon} n\Delta t, & \text{if } v_{\text{switch}} < \varepsilon \end{cases}
\end{aligned} \tag{31}$$

where

$$\begin{aligned}
t_{\text{switch}} &= \min_{n:d_{n-\tau/\Delta t} \leq d_{\text{dense}}} n\Delta t, \\
d_{\text{switch}} &= d_{t_{\text{switch}}/\Delta t}, v_{\text{switch}} = v_{t_{\text{switch}}/\Delta t}.
\end{aligned}$$

Proof: Please see the proof for *Proposition 4* in the Appendix. □

V. THE RSD ALGORITHM: PSO BASED ON RESPONSE FOR DOUBLE OBJECTIVES AND CONSTRAINTS

As per the analysis of d_{end} and t_{end} presented in Section IV, the correspondences between these parameters (d_{end} and t_{end}) and the optimization variables (a, b, d_{dense} and d_{sparse}) in **P** are uniquely determined. To overcome the intractability of **P**, a solution framework with low complexity must be designed to obtain the approximate solution. PSO is a widely used optimization algorithm proposed by Kennedy and Eberhart [34], which can optimize multiple parameters simultaneously with a fast convergence rate and low complexity [13], [35]. Therefore, as **P** is an NP-hard problem comprising four optimization variables, PSO is utilized in this paper. However, there are two differences compared with traditional PSO problems. First, there are two objectives, rather than one, in **P**. Second, there are constraints existing in **P**. To address these differences, a particular fitness function must be properly designed. Thus, the lexicographic method [36] is introduced, as it is able to guarantee performance in a sequence of the importance of objectives. Additionally, a penalty function [37] is introduced to transform the constrained optimization problem **P** into an unconstrained optimization problem so that each particle can have a corresponding fitness value in PSO.

This section proposes a solution framework called the reduction of standstill spacing and braking duration (RSD) algorithm, which utilizes PSO combined with the lexicographic method and penalty function. The design of the fitness function in the proposed RSD algorithm to evaluate particles is introduced in subsection V-A. Then, subsection V-B presents the workflow of the proposed RSD algorithm.

A. FITNESS FUNCTION FOR DOUBLE OBJECTIVES AND CONSTRAINTS

A fitness function is designed to address the multiple objectives and constraints in **P**. First, $\mathbf{x}$ is set as the iteration variable, and fv is set as the fitness value in the PSO fitness function As there are four optimization variables in **P**, including a, b, d_{dense} and d_{sparse} the form of vector $\mathbf{x}$ is $\mathbf{x} = (a, b, d_{\text{dense}}, d_{\text{sparse}})$.

1) THE LEXICOGRAPHIC METHOD FOR SEQUENCE OPTIMIZATION AND THE PENALTY FUNCTION FOR TRANSFORMING THE CONSTRAINTS

As **P** is a double-objective optimization problem the lexicographic method [36] is introduced by optimizing two single-objective subproblems in the sequence of importance. In this paper, compared with t_{end}, d_{end} is closely related to road utilization and safety insurance. Therefore, d_{end} is taken as the first objective, and t_{end} is the second objective. Then, **P** is optimized by solving two suboptimization problems in sequence, named Sub-P1 and Sub-P2. For the former Sub-P1, its objective is min d_{end}, and its constraints correspond to the constraints (a-e) in **P**, where constraint (a) is transformed into $d_{\text{end}} \geq d_{\text{safe}}$. This is because $d(t)$ decreases monotonically and d_{end} is the minimum value of $d(t)$. Here, d_{opt} represents the minimal objective value in optimizing Sub-P1. For the latter suboptimization problem Sub-P2, after the optimization of Sub-P1, t_{end} is optimized. To guarantee the performance of the first objective d_{end} in the subsequent optimization, the constraint $d_{\text{end}} \leq (1 + rel)d_{\text{opt}}$ is added in Sub-P2, where rel denotes a relaxation to guarantee that Sub-P2 is convex and solved efficiently and within a suitable time frame [36]. Thus, the constraints of Sub-P2 correspond to constraints (a-e), where constraint (a) is transformed into $d_{\text{safe}} \leq d_{\text{end}} \leq (1+rel)d_{\text{opt}}$. Based on the preceding analysis, an independent variable $flag$ is introduced as an indicator to indicate whether d_{end} in Sub-P1 ($flag = 1$) or t_{end} in Sub-P2 ($flag = 2$) is obtained.

As constraints exist in Sub-P1 and Sub-P2, the iterative process in PSO cannot be directly executed. Thus, the penalty function is introduced to impart a large penalty value λ to the particles that do not satisfy the constraints in Sub-P1 and Sub-P2 [37] because both Sub-P1 and Sub-P2 are minimization problems. This can transform the constrained **P** into an unconstrained optimization problem for the execution of PSO. In addition, combined with the subproblem indicator $flag$, the fitness function $F(.)$ is represented as follows:

$$fv = F(\mathbf{x}, \lambda, flag) = \begin{cases} d_{\text{end}}(t_{\text{end}}), & \text{if the constraints are satisfied} \\ \lambda, & \text{if the constraints are not satisfied} \end{cases} \tag{32}$$

2) THE DESIGNED FITNESS FUNCTION

As PM1 stops in Braking stage 1 in Braking scenario 1, and it stops in Braking stage 2 in Braking scenario 2, the determination of d_{end} and t_{end} in Braking scenario 1 is based on *Proposition 3*, while that in Braking scenario 2 is based on *Proposition 4* by obtaining d_{switch} and v_{switch} based on *Proposition 2*. Then, based on the above analysis, the determination of fv in Braking scenarios 1 and 2 is designed in the rest of this part.

First, the stability condition is judged for each particle by constraints (c-e) in **P**. Next, for stable particles, the *crossing criterion* is introduced to obtain fv in Braking scenarios 1 and 2, respectively.

Next, for the in-vehicle safety, the judgment corresponds to constraint (b) in Sub-P1 and Sub-P2, i.e., $s(t) \leq s_{\max}$. Because v_n can be obtained by the introduced RK4, the deceleration at t_n can be approximated and judged as

$$s_n = -u_n = -\frac{v_n - v_{n-1}}{t_n - t_{n-1}} = \frac{v_{n-1} - v_n}{\Delta t} \leq s_{\max}, \tag{33}$$

where s_n represents the approximate value of $s(t_n)$.

Here, t_n should be from $-\tau$ to $t_{\max}$, $t_{\max}$ is an input denoted as the maximum permissible time for braking, and $L = \lfloor t_{\max}/\Delta t \rfloor$.

For inter-vehicle safety, constraint (a) in Sub-P1 and Sub-P2 must be judged as follows:

$$d_{\text{safe}} \leq d_{\text{end}}, \quad \text{if } flag = 1 \tag{34a}$$

$$d_{\text{safe}} \leq d_{\text{end}} \leq (1 + rel)d_{\text{opt}}, \quad \text{if } flag = 2 \tag{34b}$$

If the string stability is ensured, the in-vehicle and inter-vehicle safety are satisfied, and we have $fv = d_{\text{end}}$, if $flag = 1$, and $fv = t_{\text{end}}$, if $flag = 2$. Otherwise, if any one of the constraints is not satisfied, $fv = \lambda$.

The determination of the fitness function is described in Algorithm 1.

B. THE PROPOSED RSD ALGORITHM

The proposed RSD algorithm based on PSO is subsequently presented in detail. The symbols used in PSO are listed in Table 1. The procedures of the proposed RSD algorithm are then presented.

TABLE 1. Summary of notations in the PSO algorithm.

Notation	Description
N	Number of particles
K	Number of iterations
$\mathbf{x}_{\min}$, $\mathbf{x}_{\max}$	Upper and lower limits of the positions of particles
$\mathbf{v}_{\min}$, $\mathbf{v}_{\max}$	Upper and lower limits of the velocities of particles
c_1, c_2	Learning factors 1 and 2
ω	Inertia of particles

Here, the complexity of the proposed RSD algorithm is polynomial $O(LNK)$. Please see the proof of the complexity computation in the Appendix.

VI. SIMULATION RESULTS

This section consists of three parts. Subsection VI-A demonstrates the accuracy of the analysis of standstill spacing and braking duration by the DDEs, including the *crossing criterion* and the determination of d_{end} and t_{end} based on RK4. Next, in subsection VI-B, the improved performance of the proposed RSD algorithm is presented via comparison with four related algorithms, namely, the car-following algorithm [25], the feedback control algorithm [26], the maximum braking algorithm [27], and the fixed setting algorithm using

Algorithm 1 Construction of the Fitness Function $fv = F(\mathbf{x}, \lambda, flag)$

Inputs: $\mathbf{x}$, λ, $flag$, $v_{\max}$, v_{stable}, d_{safe}, $s_{\max}$, ε, Δt, τ, rel, L
Output: $fv = F(\mathbf{x}, \lambda, flag)$

Initialize $fv = \lambda$
if the platoon is string stable based on constraints (c–e) in **P** // ensure string stability **then**
  Obtain d_{stable} based on Eq. (3)
  Obtain d_n and v_n for $n = -\tau/\Delta t, \ldots, 0$ based on *Proposition 1*
  for each t_n, $n = 1, 2, 3, \ldots, L$ **do**
    Obtain d_n and v_n based on *Proposition 2*
    if Inequality (33) is satisfied // ensure in-vehicle safety **then**
      if the braking process belongs to Braking scenario 1 based on *crossing criterion* **then**
        if $v_n \le \varepsilon$ **then**
          $d_{\text{end}} = d_{\text{dense}}$ and $t_{\text{end}} = n\Delta t$
          Goto Step 23
        end if
      else
        if $d_{n-\tau}/\Delta t < d_{\text{dense}}$ **then**
          Obtain d_{end} and t_{end} based on *Proposition 4*.
          Goto Step 23
        end if
      end if
    else
      Goto Step 26
    end if
  end for
  if Inequality (34) is satisfied // ensure inter-vehicle safety **then**
    Obtain fv based on $flag$
  end if
end if

Algorithm 2 The Proposed RSD Algorithm

Inputs: N, K, $\mathbf{x}_{\min}$, $\mathbf{x}_{\max}$, $\mathbf{v}_{\min}$, $\mathbf{v}_{\max}$, c_1, c_2, ω.

1: Conduct PSO where the fitness function is $fv = F(\mathbf{x}, \lambda, 1)$ and the optimization objective is $\min d_{\text{end}}$.
2: After PSO in step 1, it can be obtained that $d_{\text{opt}} = F(\mathbf{x}_{\text{gbest}}, \lambda, 1)$
3: Conduct PSO where the fitness function is $fv = F(\mathbf{x}, \lambda, 2)$ and the optimization objective is $\min t_{\text{end}}$. Here, d_{opt} is introduced in this step because constraint (a) in $fv = F(\mathbf{x}, \lambda, 2)$ is $d_{\text{safe}} \le d_{\text{end}} \le (1 + rel)d_{\text{opt}}$ to illuminate particles that cannot guarantee the performance of the first objective d_{end} in step 1.

Outputs: $d_{\text{end}} = F(\mathbf{x}_{\text{gbest}}, \lambda, 1)$, $t_{\text{end}} = F(\mathbf{x}_{\text{gbest}}, \lambda, 2)$, results of optimization variables $\mathbf{x}_{\text{gbest}}$.

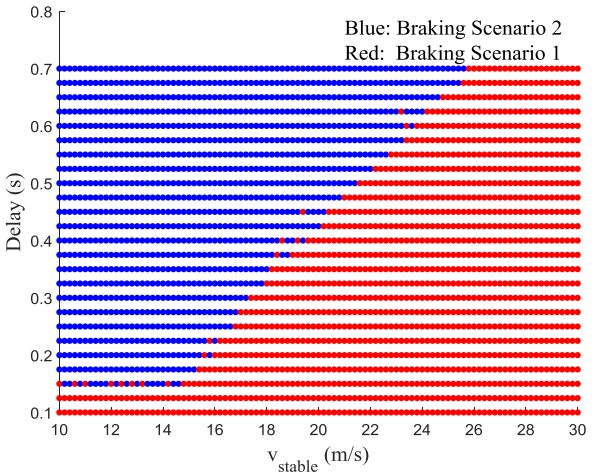

FIGURE 4. Actual distribution of Braking scenarios 1 and 2.

the same control laws [6]. Finally, in subsection VI-C, the relationship among the limits of the stable velocity, the delay and the stable distance is presented as a reference for platoon control while ensuring safety.

A. THE ACCURACY OF MODELING THE BRAKING PROCESS

1) CROSSING CRITERION

A *crossing criterion* defined in Section IV-B is proposed to divide the braking process into Braking scenario 1 and Braking scenario 2, and its accuracy is subsequently verified

Fig. 4 presents the actual results of the classification of braking scenarios with different delays and stable velocities, in which it can be seen that the percent of braking in Braking scenario 1 is greater with shorter delays and larger values of v_{stable}. In addition, the braking process tends to be Braking scenario 1 when the delays are close to 0. This is because when delays are close to 0, the DDE (8) of Braking stage 1 tends to be an ODE, the solution of which is nonoscillatory and decreasing, i.e., the braking process belongs to Braking scenario 1 when $\tau = 0$.

As shown in Fig. 5, PM1 has a longer d_{stable} to brake when it drives with a higher value of v_{stable}, and the braking process tends to be Braking scenario 1. Therefore, a shorter time delay and larger d_{stable} make the braking process more relaxed.

Fig. 6 presents the accuracy of the *crossing criterion* with different delays and stable velocities. For each point in Fig. 6, the optimization variables including a, b, d_{dense}, and d_{sparse}, are optimized by the proposed RSD algorithm. The accuracy of the *crossing criterion* is found to be 94.02%. The distribution of inaccurate points of the *crossing criterion* is close to a line (represented by blue dots) because the value of $f(z_0)$ corresponding to this line is close to 0, leading to the inaccuracy of the *crossing criterion*.

2) THE DETERMINATION OF d_{end} AND t_{end}

Fig. 7 presents the percentage of differences between the theoretical and simulated values for d_{end} and t_{end}. As presented in Fig. 7(a), the percentage of differences for d_{end} is less than

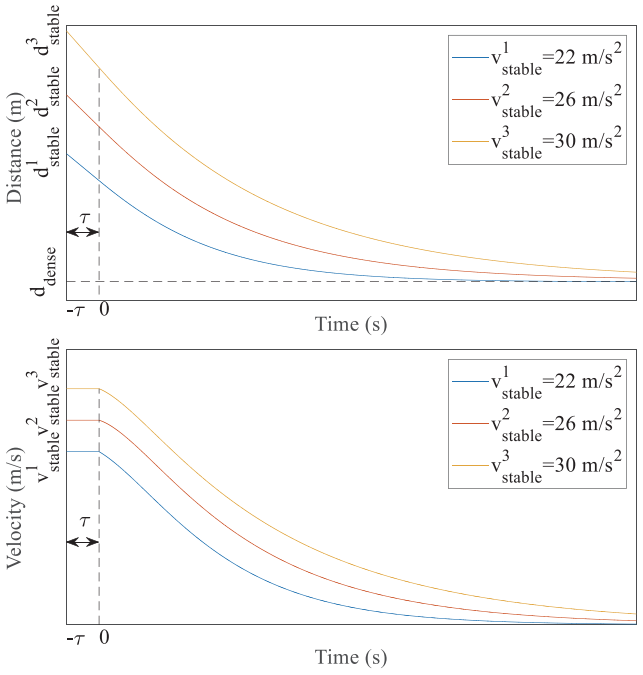

FIGURE 5. PM1 braking with different values of v_{stable} under the same delay.

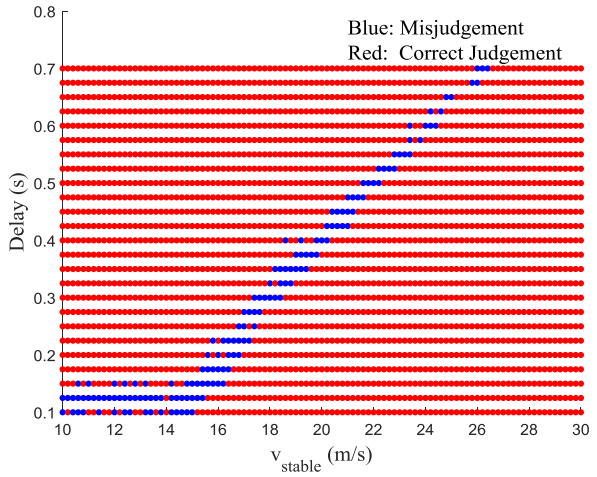

FIGURE 6. Accuracy of *crossing criterion*.

0.18%, while that for t_{end} is less than 0.03%, as presented in Fig. 7(b). Thus, the propositions for the determination of d_{end} and t_{end} are highly accurate.

B. THE PERFORMANCE OF THE PROPOSED RSD ALGORITHM

To evaluate the performance of the proposed RSD algorithm, it is compared with four related algorithms, namely, the car-following algorithm [25], the feedback control algorithm [26] the maximum braking algorithm [27], and the fixed setting algorithm, which has the same control laws as the RSD algorithm. The parameters are listed in Table 2, and the parameters of the fixed setting algorithm are set as $a = 4, b = 0.6, d_{\text{sparse}} = 35$ m, and $d_{\text{dense}} = 1.5d_{\text{safe}}/d_{\text{dense}} = 2d_{\text{safe}}$ [6].

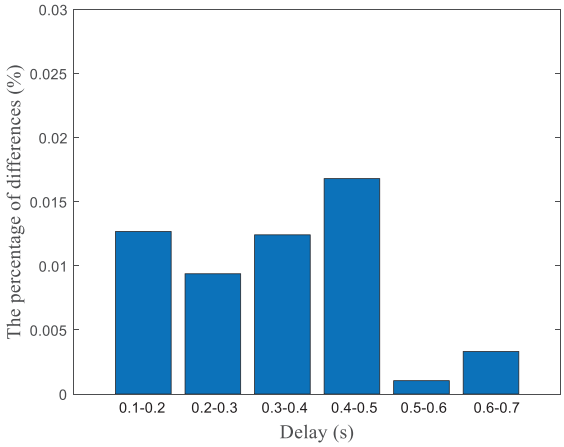

(a) Standstill spacing.

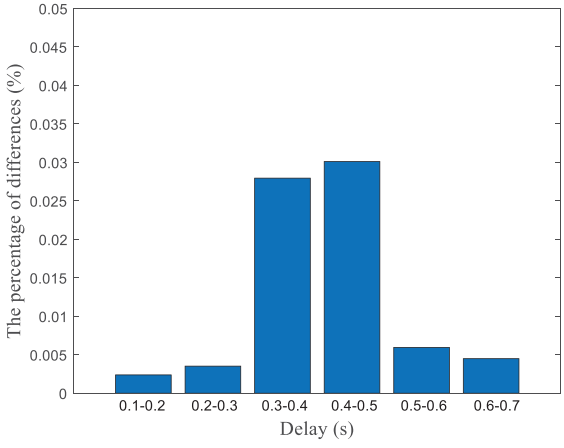

(b) Braking duration.

FIGURE 7. The percentage of differences between the theoretical and simulated values.

TABLE 2. Simulation parameters.

Symbol	Value	Symbol	Value
$v_{\max}$	30 m/s	N	100
v_{stable}	15 m/s	T	40
d_{safe}	6 m	ω	0.9
$s_{\max}$	10 m/s^2	c_1	1.5
ε	0.1 m/s	c_2	1.5
$\mathbf{v}_{\max}$	$(0.5, 0.2, 4, 4)$	$\mathbf{x}_{\max}$	$(20, 0.6667, 40, 100)$
$\mathbf{v}_{\min}$	$(-0.5, -0.2, -4, -4)$	$\mathbf{x}_{\min}$	$(0, 0, 6, 40)$
λ	10000	*rel*	0.1
$t_{\max}$	5 s		

PM1 starts to brake at t_{brake}; hence, $s(0)$ can be derived as

$$\begin{aligned} s(0) &= -u(0) \\ &= -(a\,[V(d(t_{\text{brake}} - \tau)) - v_1(0)] \\ &\quad + b[v_0(t_{\text{brake}} - \tau) - v_1(0)]) \\ &= -\left(a\,[V(d(-\tau)) - v_1(0)] + b\,[v_0(-\tau) - v_1(0)]\right) \\ &= bv_{\text{stable}} \end{aligned} \tag{35}$$

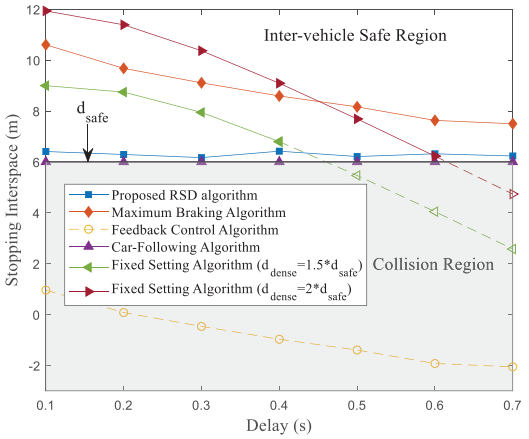

(a) Standstill spacing.

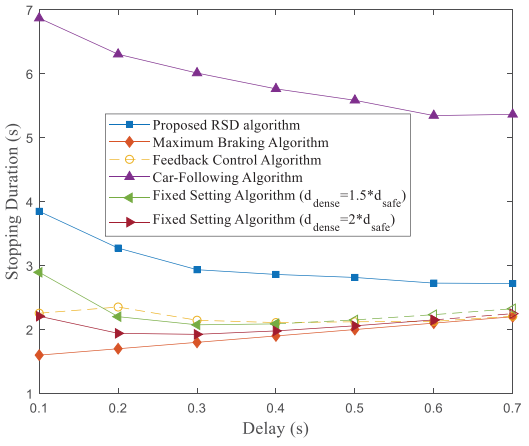

(b) Braking duration.

FIGURE 8. Comparison of standstill spacing and braking duration.

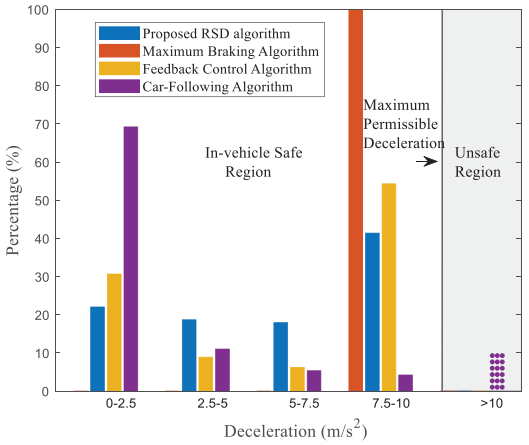

(a) Distribution of deceleration.

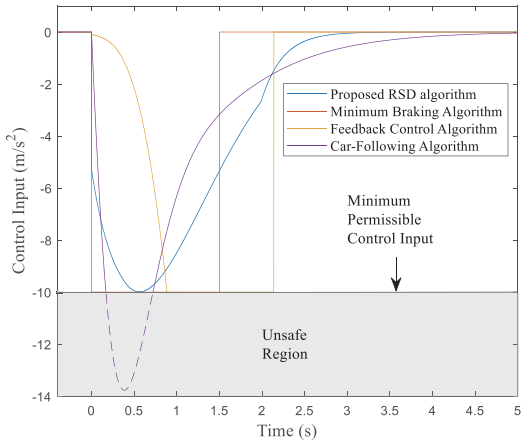

(b) Control input dependent on time when $\tau = 0.4$ s.

FIGURE 9. Comparison of deceleration and control input.

For the constraint $s(t) \leq s_{\max}$, it should be ensured that $bv_{\text{stable}} \leq s_{\max}$. Therefore, $b \leq u_{\max}/v_{\text{stable}}$, and the maximum deceleration value for a vehicle is 10 m/s^2 [38].

The maximum value of d_{sparse} is 100 m because the maximum safe distance between vehicles for a platoon requires d_{stable} to be 100 m [39] when it drives at a speed of 30 m/s. In addition, $\min d_{\text{sparse}} \geq \max d_{\text{dense}}$, or the control law (2) will not work if $d_{\text{sparse}} < d_{\text{dense}}$.

Furthermore, the control gains a and b must be guaranteed as $a > 0$ and $b > 0$ so that $\min a = \min b = 0$.

Fig. 8 illustrates the standstill spacing and braking duration under different delays, which represent inter-vehicle safety (Fig. 8(a)) and road utilization (Figs. 8(a) and 8(b)). It is evident that the fixed setting algorithm and the feedback control algorithm cannot guarantee inter-vehicle safety, i.e., $d_{\text{end}} < d_{\text{safe}}$ and the unsafe results are represented as hollow points. For the fixed setting algorithm, it is found that d_{end} decreases with the increase of delays, and it finally induces collision with a high delay ($\tau > 0.5$ s for $d_{\text{dense}} = 1.5d_{\text{safe}}$, $\tau > 0.6$ s for $d_{\text{dense}} = 2d_{\text{safe}}$) because the fixed control parameters in control laws (1) and (2) cannot cope with the worsened delay condition. The feedback control algorithm lacks both the offset of delay in distance estimation and adequate deceleration.

Fig. 9 demonstrates the distribution of deceleration under different delays and control input dependent on time when $\tau = 0.4$ s, which represents in-vehicle safety. It is noted that deceleration is equal to the absolute value of control input, so that deceleration is greater than 0 and control input is less than 0. It is clear that the car-following algorithm cannot guarantee in-vehicle safety, i.e., $s > s_{\max}$ and the unsafe results are represented as hollow columns and dotted lines. This is because the insurance of in-vehicle safety is not considered in the car-following algorithm, which uses an overly large deceleration in the decelerating phase. In addition, Fig. 8(b) shows that the braking duration in the proposed RSD algorithm is less than 4 s, while that in the car-following algorithm ranges from 5.2 s to 7 s. In other words, it has a longer braking duration compared with the proposed algorithm, even though it exceeds the limit of deceleration in the decelerating phase.

It is evident in Figs. 8 and 9 that, aside from the proposed RSD algorithm, only the maximum braking algorithm can ensure safety, and it is found to have a shorter braking duration based on Fig. 8(b). However, the standstill spacing in

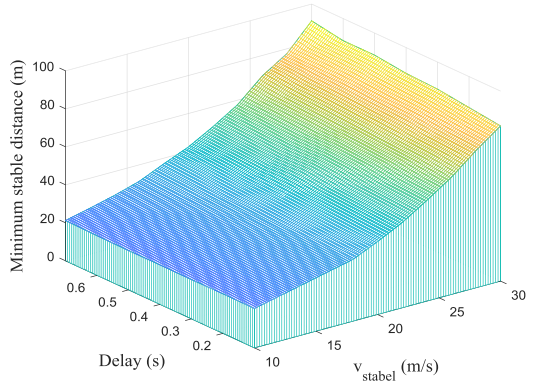

FIGURE 10. The minimum stable distance for ensuring safety (d_{safe} = 6 m).

the maximum braking algorithm is greater than 8 m based on Fig. 8(a), which is not beneficial for improving road utilization. Moreover, under this algorithm, the vehicles will continuously brake at the maximum deceleration based on Fig. 9(a), and the control input will experience a sudden fall and rise at the beginning and end of the braking process based on Fig. 9(b), which will have a sharp and substantial impact on passengers, who will be made to feel extremely uncomfortable. In summary, only the proposed RSD algorithm can simultaneously improve road utilization and ensure the two aspects of safety.

C. RESULTS FOR REFERENCE

The relationship among the limits of the stable velocity, the delay, and the stable distance is presented for reference in platoon control while ensuring safety.

Fig. 10 presents the minimum stable distance for ensuring safety at different delays and stable velocities. If the stable distance is shorter than the minimum value, the standstill spacing may be less than the safe distance, or the deceleration may be beyond the permissible value. In Fig. 10, it can be seen that the minimum stable distance increases with the stable velocity and delay because a longer distance is required to safely brake when vehicles drive at higher speeds or under longer delays.

VII. CONCLUSION

This paper proposes an optimized braking control under delays in which road utilization is improved by reducing the standstill spacing and braking duration while ensuring safety. In particular, the braking process is modeled using DDEs to embed the effect of delay. In addition, a crossing criterion is introduced to classify the braking scenarios. Furthermore, the time functions of the distance and velocity during braking are derived, and propositions of the standstill spacing and braking duration are made based on the Runge-Kutta method. Then, under the consideration of ensuring safety with delays, the road utilization is improved via the optimization of the control parameters, and a solution framework with polynomial complexity $O(LNK)$ is provided. The simulation results verify the accuracy of the braking modeling process, demonstrate the performance of the proposed algorithm, and provide results as a reference for platoon control.

Furthermore, braking with time-variant delays, heterogeneous platoons and different information topologies can be studied in the future. Moreover, the lateral behavior of a platoon during the braking process will be considered in the future

APPENDIX A
PROOF OF PROPOSITION 2

Proof: The initial value problem for the DDE (28) is as follows:

$$\begin{aligned} \mathbf{y}'(t) &= \mathbf{L}\mathbf{y}(t) + \mathbf{M}\mathbf{y}(t-\tau) + \boldsymbol{N} \\ \mathbf{y}(t) &= \mathbf{P}t + \mathbf{Q}, \quad t \le 0 \end{aligned} \tag{36}$$

where $\mathbf{y}(t) = \mathbf{P}t + \mathbf{Q}$ is the initial function of the DDE.

Here, $(t_n, \mathbf{y}_n)$ denotes the n-th value of $(t, \mathbf{y})$, and this is required to obtain the value of $(t_n, \mathbf{y}_n)$ for $t_n > 0$, where $t = 0$ represents the initial moment of the equation.

The formula of the approximate solution of the DDE is as follows [40]:

$$\mathbf{y}_{n+1} = \mathbf{y}_n + \Delta t \sum_{i=1}^{s} h_i \mathbf{f}_{ni} \tag{37a}$$

$$t_{n+1} = t_n + \Delta t \tag{37b}$$

where $\mathbf{f}_{ni}$ denotes the i-th approximate growth rate of $(t_n, \mathbf{y}_n)$, h_i is the weight of $\mathbf{f}_{ni}$, and s represents the order of the method, $n = 0, 1, 2, \ldots$.

Then f_{ni} can be derived as follows [40].

$$\begin{aligned} \mathbf{f}_{ni} &= \mathbf{L}\mathbf{y}_{ni} + \mathbf{M}\mathbf{S}(t_{ni} - \tau) + \boldsymbol{N} \\ t_{ni} &= t_n + \Delta t c_i, \quad i = 1, \ldots, s \\ \mathbf{y}_{ni} &= \mathbf{y}_n + \Delta t \sum_{j=1}^{i-1} a_{ij} \mathbf{f}_{nj} \end{aligned} \tag{38}$$

Note that $\mathbf{S}(t_{ni} - \tau)$ denotes the approximate, not the exact, value of $\mathbf{y}(t_{ni} - \tau)$. Thus, $\mathbf{S}(t_{ni} - \tau)$ is different from $\mathbf{y}(t_{ni} - \tau)$. Because Δt is a step factor of τ in the proposed algorithm, i.e., $q = \tau/\Delta t$, and q is an integer, $(t_{ni} - \tau, \mathbf{y}(t_{ni} - \tau))$ is approximated by $(t_{ni-q}, \mathbf{y}_{ni-q}), n = 0, 1, 2, \ldots$. Hence, $\mathbf{S}(t_{ni} - \tau)$ is equal to $\mathbf{y}_{ni-q}$.

Based on the preceding analysis, the formula of RK4 can be obtained as *Proposition 2* [40].

It is noted that $y_n = \mathbf{P}(n\Delta t) + \mathbf{Q}$ and $\mathbf{k}_{n,i} = d(\mathbf{P}(n\Delta t) + \mathbf{Q})/dt$ when $n \le 0, i = 1, 2, 3$, i.e., $\mathbf{y}_n$ and $\mathbf{k}_{n,i}$ are exact values when $n \le 0$ because the initial function is given, in which $\mathbf{k}_{n,i} (n \le 0, i = 1, 2, 3)$ are equal. □

APPENDIX B
PROOF OF PROPOSITION 3

Proof: In Braking scenario 1, the forms of $d(t)$ and $v(t)$ are obtained as follows based on Eqs. (12a) and (15):

$$d(t) = Ae^{-zt} + d_{\text{dense}} \tag{39a}$$

$$v(t) = zAe^{-zt} \tag{39b}$$

i.e., $d(t)$ will decrease to d_{dense}, $v(t)$ will decrease to 0, and $d_{\text{end}} = d_{\text{dense}}$.

Based on the analysis of Braking scenario 1 in Section IV-C, the braking process ends if $v(t) \leq \varepsilon$. Therefore, $t_{\text{end}} = n\Delta t$ when it enters $v_n \leq \varepsilon$, i.e., $t_{\text{end}} = \min_{n:v_n \leq \varepsilon} n\Delta t$, because $v(t)$ decreases monotonously with time, i.e., $v_n > \varepsilon$ if $n < t_{end}/\Delta t$ and $v_n \leq \varepsilon$ if $n \geq t_{end}/\Delta t$. □

APPENDIX C
PROOF OF PROPOSITION 4

Proof: When $t \geq t_{\text{switch}}$, the equations of $d(t)$ and $v(t)$ are (11a) and (11b), respectively. Thus, $d(t)$ and $v(t)$ will be uniquely identified after t_{switch} if t_{switch}, d_{switch}, and v_{switch} are given.

Based on the analysis presented in Section IV-A, t_{dense} is the moment at which $d(t) = d_{\text{dense}}$, i.e., $d(t) > d_{\text{dense}}$ if $t < t_{\text{dense}}$ and $d(t) < d_{\text{dense}}$ if $t > t_{\text{dense}}$. In other words, $d(t) > d_{\text{dense}}$ if $t < t_{\text{switch}} - \tau$ and $d(t) < d_{\text{dense}}$ if $t > t_{\text{switch}} - \tau$, as $t_{\text{dense}} = t_{\text{switch}} - \tau$. Thus, $t_{\text{switch}} = \min_{n:d_{n-\tau/\Delta t} \leq d_{\text{dense}}} n\Delta t$ according to the proof of *Proposition 3*. In addition, $v_{\text{switch}} = v_n$ and $d_{\text{switch}} = d_n$ at moment $t = t_{\text{switch}}$, i.e., $n = t_{\text{switch}}/\Delta t$. Therefore, t_{switch}, d_{switch}, and v_{switch} are obtained in Braking stage 1 through *Proposition 2*.

Here, $d(t)$ in Braking stage 2 decreases to $d_{\text{switch}} - \frac{v_{\text{switch}}}{a+b}$ so that $d_{\text{end}} = d_{\text{switch}} - \frac{v_{\text{switch}}}{a+b}$ according to the proof of *Proposition 3*.

Because PM1 is considered to stop if $v(t) \leq \varepsilon$, there are two cases for the determination of t_{end}, as $v(t) \leq \varepsilon$ will be in Braking stage 1 or 2.

Case 1: $v(t) \leq \varepsilon$ is in Braking stage 1. In this case, $v_{\text{switch}} < \varepsilon$ because v_{switch} is the final velocity of Braking stage 1. Thus, $t_{\text{end}} = \min_{n:v_n \leq \varepsilon} n\Delta t$ based on the proof of *Proposition 3*.

Case 2: $v(t) \leq \varepsilon$ is in Braking stage 2. In this case, $v_{\text{switch}} \geq \varepsilon$ because v_{switch} is the initial velocity of Braking stage 2. Because $v(t)$ is decreasing in Braking stage 2, t_{end} is obtained by solving the following equation:

$$v_{\text{switch}} e^{(a+b)(t_{\text{switch}} - t_{\text{end}})} = \varepsilon \tag{40}$$

so that

$$t_{\text{end}} = t_{\text{switch}} + \frac{\ln v_{\text{switch}} - \ln \varepsilon}{a+b} \tag{41}$$

□

APPENDIX D
PROOF OF COMPLEXITY COMPUTATION

When computing the complexity, the order of magnitude of the most executed statements is equal to the complexity. In the RSD algorithm, the innermost loop is the obtaining of d_{end} or t_{end} in the fitness function, which should be executed at most L times. Then, in the PSO process, N particles will be updated K times, and one update contains the obtaining of d_{end} or t_{end} at most L times.

Based on the above analysis, d_{end} or t_{end} will be obtained at most LNK times; namely, the complexity is $O(LNK)$, and it is polynomial complexity.

REFERENCES

[1] D. Jia, K. Lu, J. Wang, X. Zhang, and X. Shen, "A survey on platoon-based vehicular cyber-physical systems," *IEEE Commun. Surveys Tuts.*, vol. 18, no. 1, pp. 263–284, 1st Quart., 2016.

[2] C. Bergenheim, S. Shladover, E. Coelingh, C. Englund, and S. Tsugawa, "Overview of platooning systems," in *Proc. World Congr.*, 2012, pp. 1–8.

[3] A. S. A. Rachman, A. F. Idriz, S. Li, and S. Baldi, "Real-time performance and safety validation of an integrated vehicle dynamic control strategy," *IFAC-PapersOnLine*, vol. 50, no. 1, pp. 13854–13859, Jul. 2017.

[4] J. C. Zegers, E. Semsar-Kazerooni, J. Ploeg, N. van de Wouw, and H. Nijmeijer, "Consensus-based bi-directional CACC for vehicular platooning," in *Proc. Amer. Control Conf. (ACC)*, Jul. 2016, pp. 2578–2584.

[5] E. Semsar-Kazerooni, J. Verhaegh, J. Ploeg, and M. Alirezaei, "Cooperative adaptive cruise control: An artificial potential field approach," in *Proc. IEEE Intell. Vehicles Symp. (IV)*, Jun. 2016, pp. 361–367.

[6] T. Zeng, O. Semiari, W. Saad, and M. Bennis, "Joint communication and control for wireless autonomous vehicular platoon systems," *IEEE Trans. Commun.*, vol. 67, no. 11, pp. 7907–7922, Nov. 2019.

[7] Y. Wang, Z. Zhou, C. Wei, Y. Liu, and C. Yin, "Host–target vehicle model-based lateral state estimation for preceding target vehicles considering measurement delay," *IEEE Trans. Ind. Informat.*, vol. 14, no. 9, pp. 4190–4199, Sep. 2018.

[8] D. Dileep, M. Fusco, J. Verhaegh, L. Hetel, and W. Michiels, "Achieving an L2 string stable one vehicle look-ahead platoon with heterogeneity in time-delays," in *Proc. 18th Eur. Control Conf. (ECC)*, 2019, pp. 1220–1226.

[9] S. Wei, Y. Zou, X. Zhang, T. Zhang, and X. Li, "An integrated longitudinal and lateral vehicle following control system with radar and vehicle-to-vehicle communication," *IEEE Trans. Veh. Technol.*, vol. 68, no. 2, pp. 1116–1127, Feb. 2019.

[10] X. Liu, A. Goldsmith, S. S. Mahal, and J. K. Hedrick, "Effects of communication delay on string stability in vehicle platoons," in *Proc. IEEE Intell. Transp. Syst. (ITSC)*, Aug. 2001, pp. 625–630.

[11] M. di Bernardo, A. Salvi, and S. Santini, "Distributed consensus strategy for platooning of vehicles in the presence of time-varying heterogeneous communication delays," *IEEE Trans. Intell. Transp. Syst.*, vol. 16, no. 1, pp. 102–112, Feb. 2015.

[12] M. di Bernardo, P. Falcone, A. Salvi, and S. Santini, "Design, analysis, and experimental validation of a distributed protocol for platooning in the presence of time-varying heterogeneous delays," *IEEE Trans. Control Syst. Technol.*, vol. 24, no. 2, pp. 413–427, Mar. 2016.

[13] H. Chehardoli, "Robust optimal control and identification of adaptive cruise control systems in the presence of time delay and parameter uncertainties," *J. Vib. Control*, vol. 26, nos. 17–18, pp. 1590–1601, Sep. 2020.

[14] Y. Li, C. Tang, S. Peeta, and Y. Wang, "Nonlinear consensus-based connected vehicle platoon control incorporating car-following interactions and heterogeneous time delays," *IEEE Trans. Intell. Transp. Syst.*, vol. 20, no. 6, pp. 2209–2219, Jun. 2019.

[15] A. F. Idriz, A. S. A. Rachman, and S. Baldi, "Integration of auto-steering with adaptive cruise control for improved cornering behaviour," *IET Intell. Transp. Syst.*, vol. 11, no. 10, pp. 667–675, Dec. 2017.

[16] L. Xu, W. Zhuang, G. Yin, C. Bian, and H. Wu, "Modeling and robust control of heterogeneous vehicle platoons on curved roads subject to disturbances and delays," *IEEE Trans. Veh. Technol.*, vol. 68, no. 12, pp. 11551–11564, Dec. 2019.

[17] B. Besselink and K. H. Johansson, "String stability and a delay-based spacing policy for vehicle platoons subject to disturbances," *IEEE Trans. Autom. Control*, vol. 62, no. 9, pp. 4376–4391, Sep. 2017.

[18] C. Zou and H. Li, "Event-driven connected vehicular platoon control with mixed time-varying delay," *IEEE Access*, vol. 7, pp. 111477–111486, 2019.

[19] B. Tian, X. Deng, Z. Xu, Y. Zhang, and X. Zhao, "Modeling and numerical analysis on communication delay boundary for CACC string stability," *IEEE Access*, vol. 7, pp. 168870–168884, 2019.

[20] Y. Liu, C. Pan, H. Gao, and G. Guo, "Cooperative spacing control for interconnected vehicle systems with input delays," *IEEE Trans. Veh. Technol.*, vol. 66, no. 12, pp. 10692–10704, Jun. 2017.

[21] Y. Li, C. Tang, S. Peeta, and Y. Wang, "Integral-sliding-mode braking control for a connected vehicle platoon: Theory and application," *IEEE Trans. Ind. Electron.*, vol. 66, no. 6, pp. 4618–4628, Jun. 2019.

[22] Y. Liu and B. Xu, "Improved protocols and stability analysis for multivehicle cooperative autonomous systems," *IEEE Trans. Intell. Transp. Syst.*, vol. 16, no. 5, pp. 2700–2710, Oct. 2015.

[23] Y. Liu, B. Xu, and Y. Ding, "Convergence analysis of cooperative braking control for interconnected vehicle systems," *IEEE Trans. Intell. Transp. Syst.*, vol. 18, no. 7, pp. 1894–1906, Jul. 2017.
[24] R. Zheng, K. Nakano, S. Yamabe, M. Aki, H. Nakamura, and Y. Suda, "Study on emergency-avoidance braking for the automatic platooning of trucks," *IEEE Trans. Intell. Transp. Syst.*, vol. 15, no. 4, pp. 1748–1757, Aug. 2014.
[25] C. Flores, P. Merdrignac, R. de Charette, F. Navas, V. Milanes, and F. Nashashibi, "A cooperative car-following/emergency braking system with prediction-based pedestrian avoidance capabilities," *IEEE Trans. Intell. Transp. Syst.*, vol. 20, no. 5, pp. 1837–1846, May 2019.
[26] L. Xu, L. Y. Wang, G. Yin, and H. Zhang, "Communication information structures and contents for enhanced safety of highway vehicle platoons," *IEEE Trans. Veh. Technol.*, vol. 63, no. 9, pp. 4206–4220, Nov. 2014.
[27] J. Thunberg, N. Lyamin, K. Sjoberg, and A. Vinel, "Vehicle-to-vehicle communications for platooning: Safety analysis," *IEEE Netw. Lett.*, vol. 1, no. 4, pp. 168–172, Dec. 2019.
[28] J. I. Ge and G. Orosz, "Optimal control of connected vehicle systems with communication delay and driver reaction time," *IEEE Trans. Intell. Transp. Syst.*, vol. 18, no. 8, pp. 2056–2070, Aug. 2017.
[29] M. Bando, K. Hasebe, A. Nakayama, A. Shibata, and Y. Sugiyama, "Dynamical model of traffic congestion and numerical simulation," *Phys. Rev. E, Stat. Phys. Plasmas Fluids Relat. Interdiscip. Top.*, vol. 51, no. 2, p. 1035, 1995.
[30] H. Chehardoli and A. Ghasemi, "Adaptive centralized/decentralized control and identification of 1-D heterogeneous vehicular platoons based on constant time headway policy," *IEEE Trans. Intell. Transp. Syst.*, vol. 19, no. 10, pp. 3376–3386, Oct. 2018.
[31] N. Toshiki, H. Tadayuki, H. Yoshiyuki, and M. Rinko, *Differential Equations With Time Lag-Introduction to Functional Differential Equations*. Tokyo, Japan: Makino Shoten, 2002.
[32] I. Gyori and G. Ladas, *Oscillation Theory of Delay Differential Equations With Applications, Clarendon*. Oxford, U.K.: Oxford Univ. Press, 1991.
[33] W. Wang, Y. Zhang, and S. Li, "Stability of continuous Runge–Kutta-type methods for nonlinear neutral delay-differential equations," *Appl. Math. Model.*, vol. 33, no. 8, pp. 3319–3329, Aug. 2009.
[34] J. Kennedy and R. Eberhart, "Particle swarm optimization," in *Proc. Int. Conf. Neural Netw. (ICNN)*, vol. 4, 1995, pp. 1942–1948.
[35] M. A. Abido, "Optimal power flow using particle swarm optimization," *Int. J. Elect. Power Energy Syst.*, vol. 24, no. 7, pp. 563–571, 2002.
[36] S. Khosravani, M. Jalali, A. Khajepour, A. Kasaiezadeh, S.-K. Chen, and B. Litkouhi, "Application of lexicographic optimization method to integrated vehicle control systems," *IEEE Trans. Ind. Electron.*, vol. 65, no. 12, pp. 9677–9686, Dec. 2018.
[37] S. Kitayama, M. Arakawa, and K. Yamazaki, "Penalty function approach for the mixed discrete nonlinear problems by particle swarm optimization," *Struct. Multidisciplinary Optim.*, vol. 32, no. 3, pp. 191–202, Sep. 2006.
[38] S. John and J. O. Pedro, "A comparative study of two control schemes for anti-lock braking systems," in *Proc. 9th Asian Control Conf. (ASCC)*, Jun. 2013, pp. 1–6.
[39] Y.-L. Chen, K.-Y. Shen, and S.-C. Wang, "Forward collision warning system considering both time-to-collision and safety braking distance," in *Proc. IEEE 8th Conf. Ind. Electron. Appl. (ICIEA)*, Jun. 2013, pp. 972–977.
[40] L. F. Shampine and S. Thompson, "Solving DDEs in MATLAB," *Appl. Numer. Math.*, vol. 37, no. 4, pp. 441–458, Jun. 2001.

YUN MENG (Member, IEEE) received the B.S. and Ph.D. degrees in communication engineering from Xidian University, Xi'an, China, in 2009 and 2015, respectively. Since 2015, she has been with the School of Electronics and Control Engineering, Chang'an University. Her main research interests include platoons, interference management, and stability in vehicular networks.

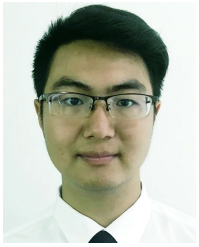

ZHUOYUAN WANG received the B.E. degree in electrical engineering and automation from Chang'an University, Xi'an, China, in 2020. He is currently pursuing the master's degree in control science and engineering with the School of Electronics and Information Engineering, Tongji University. His research interests include vehicle platoons and path and trajectory planning of agents.